

Quantum lattice representation of dark solitons

George Vahala^a, Linda Vahala^b, Jeffrey Yepez^c

^aDept. of Physics, William & Mary, Williamsburg, VA 23187

^bDept. of Electrical & Computer Engineering, Old Dominion University, Norfolk, VA 23529

^cAir Force Research Laboratory, Hanscom AFB, MA 01731

ABSTRACT

The nonlinear Schrodinger (NLS) equation in a self-defocusing Kerr medium supports dark solitons. Moreover the mean field description of a dilute Bose-Einstein condensate (BEC) is described by the Gross-Pitaevskii equation, which for a highly anisotropic (cigar-shaped) magnetic trap reduces to a one-dimensional (1D) cubic NLS in an external potential. A quantum lattice algorithm is developed for the dark solitons. Simulations are presented for both black (stationary) solitons as well as (moving) dark solitons. Collisions of dark solitons are compared with the exact analytic solutions and coupled dark-bright vector solitons are examined. The quantum algorithm requires 2 qubits per scalar field at each spatial node. The unitary collision operator quantum mechanically entangles the on-site qubits, and this transitory entanglement is spread throughout the lattice by the streaming operators. These algorithms are suitable for a Type-II quantum computers, with wave function collapse induced by quantum measurements required to determine the coupling potentials.

Keywords: dark solitons, vector dark-bright solitons, nonlinear Schrodinger equation, Gross-Pitaevskii equation, quantum lattice representation.

1. INTRODUCTION

The nonlinear Schrodinger equation (NLS) plays a pivotal role in soliton physics¹ – whether for solitons propagating in an optical fiber or for solitons in a Bose-Einstein condensate (BEC). In its simplest one-dimensional (1D) form the NLS equation for the wave function ψ is

$$i \frac{\partial \psi}{\partial t} + \frac{\partial^2 \psi}{\partial x^2} + \sigma V[|\psi|^2] \psi = 0 \quad (1)$$

where the potential $V[|\psi|^2] = |\psi|^2$ for the integrable cubic NLS. The parameter σ plays a critical role in the soliton properties : typically bright solitons exist for self-focusing ($\sigma > 0$) Kerr media while dark solitons for self-defocusing ($\sigma < 0$). For BEC dynamics (see Sec. 4 for some more details), ψ is the macroscopic wave function for the condensate and the two-particle interaction strength σ parameterizes the s-wave scattering length. This scattering length describes the elastic scattering properties of the atom-atom interaction ($\sigma > 0$ for repulsive interactions between particles in the condensate, and $\sigma < 0$ for attractive particle interactions) and can be readily tuned over orders of magnitude as well as its polarity by appropriate variations in an external magnetic field near the Feshbach resonances² (a quasi-bound molecular state at nearly zero energy coupling resonantly to the free state of the colliding atoms).

Here, we extend our earlier quantum lattice algorithms^{3,4} to the case of dark solitons (i.e., $\sigma < 0$). The simplest possible solution to the cubic defocusing NLS with $\sigma V[|\psi|^2] = -2|\psi|^2$ is the black soliton⁵

$$\psi(x,t) = a^{1/2} \text{Tanh}[a^{1/2}(x-x_0)] \text{Exp}[-2i a t] \quad (2)$$

which is a special case of the dark soliton

$$\psi(x,t) = a^{1/2} \left[\text{Tanh} \left(a^{1/2} b \left\{ x - x_0 - 2\sqrt{a(1-b^2)} t \right\} \right) + i\sqrt{1-b^2} \right] \text{Exp}[-2i a t] \quad (3)$$

with $b \rightarrow 1$. The velocity of the dark soliton is $\sqrt{a(1-b^2)}$. Unlike the bright soliton, which has two free parameters, the dark soliton only has one free parameter that couples the amplitude to its speed (the parameter a represents the background amplitude since for dark solitons, $|\psi| \rightarrow a^{1/2}$ as $|x| \rightarrow \infty$. For bright solitons, $|\psi| \rightarrow 0$ as $|x| \rightarrow \infty$). The black soliton is stationary, with $|\psi| \rightarrow 0$ at the center of the soliton and a phase jump of π across the soliton minimum

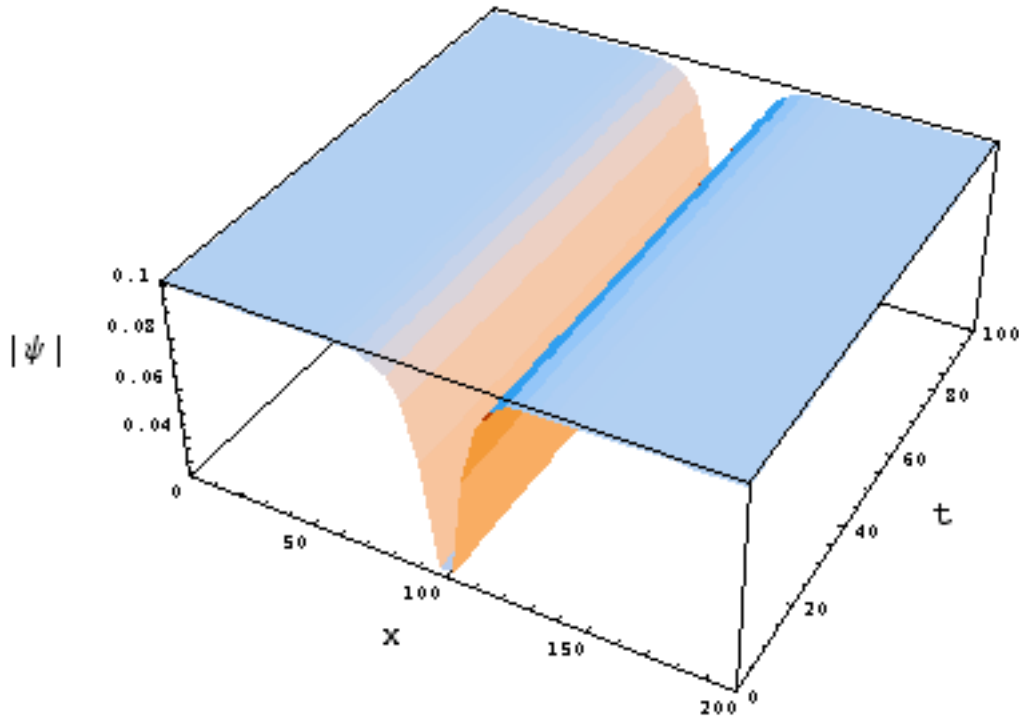


Fig. 1 A plot (both analytic and that determined from our quantum algorithm) of $|\psi|$ for the black soliton for the defocusing cubic NLS. Black solitons are stationary, with zero intensity as its minimum and a phase jump of π across its minimum. Dark solitons have a non-zero velocity, a non-zero intensity minimum with a smaller phase jump (see Fig. 6).

Of more interest is the collision of two dark solitons. An exact solution to the cubic self-defocusing NLS Schrodinger equation

$$i \frac{\partial \psi}{\partial t} + \frac{\partial^2 \psi}{\partial x^2} + \sigma V[|\psi|] \psi = 0 \quad , \quad \text{with} \quad \sigma V[|\psi|] = -2|\psi|^2 \quad (4)$$

that describes the collision of two dark solitons of equal amplitude is given by⁵

$$\psi(x,t) = -\frac{a}{2^{1/2}} \frac{\text{Cosh}(a\{x-x_0\}) + i 2^{1/2} \text{Sinh}(a^2\{t-t_0\})}{2^{1/2} \text{Cosh}(a^2\{t-t_0\}) + \text{Cosh}(a\{x-x_0\})} \text{Exp}[-i a^2 (t-t_0)] \quad (5)$$

The soliton collision dynamics is shown in Fig. 2

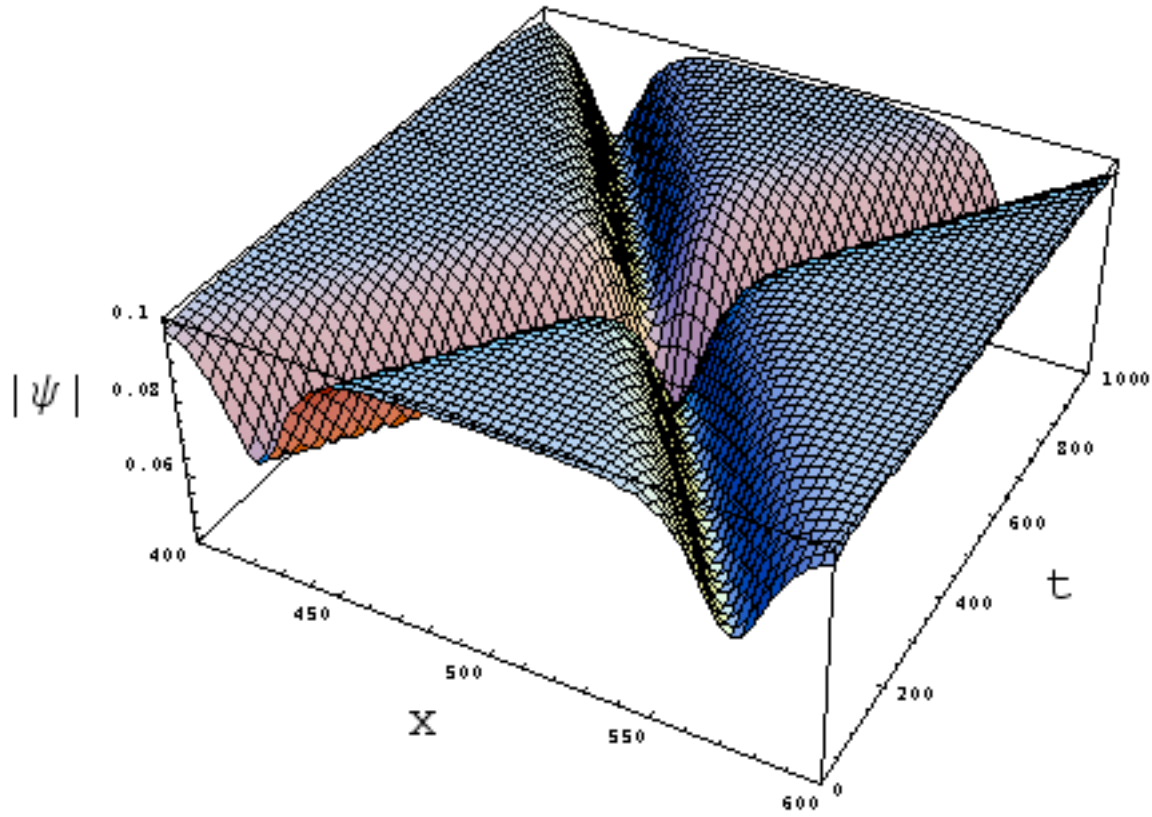


Fig. 2 The time evolution of the collision of two dark solitons of equal amplitude (for both analytic and the quantum algorithm). The spatial grid is 1000 and the number of time iterations is 1000.

Here we develop a quantum lattice algorithm for the evolution of dark solitons and their collisions as well as the vector NLS coupling of a dark-bright soliton pair under a self-defocusing nonlinearity. This is of considerable interest since the bright soliton only can exist in a defocusing medium because it is trapped within a co-propagating dark soliton. These types of interactions have been considered for an inhomogeneous two-species Bose-Einstein condensate.⁶

2. QUANTUM LATTICE REPRESENTATION FOR NLS

2.1 Scalar NLS^{3,4}

It is convenient to use the one particle sector representation of Yepez and Boghosian⁷. The spatial domain is partitioned into L spatial nodes : $x_\ell, \ell=1 \dots L$. At each spatial site we associate two qubits, $|q_1^\ell\rangle, |q_2^\ell\rangle$ for the scalar wave function ψ at x_ℓ . The simplest unitary collision operator \hat{C} that will recover Eq. (1) is a factored operator that only entangles the on-site qubits independently at each spatial site

$$\hat{C} = \otimes_{\ell=1}^L \hat{U}_\ell \tag{6}$$

A local equilibrium can be associated with this on-site unitary collision operator if $|v\rangle$ is an eigenvector of \hat{U}_ℓ with unit eigenvalue : $\hat{U}_\ell |v\rangle = |v\rangle$.

Introducing the \sqrt{SWAP} -gate on a site by site basis

$$\hat{U} = \begin{pmatrix} 1 & 0 & 0 & 0 \\ 0 & \frac{1-i}{2} & \frac{1+i}{2} & 0 \\ 0 & \frac{1+i}{2} & \frac{1-i}{2} & 0 \\ 0 & 0 & 0 & 1 \end{pmatrix} \quad \text{with } \hat{U}_\ell = \hat{U} \quad (7)$$

with the Hamiltonian tensor product representation

$$\hat{U} = \exp\left[\frac{i\pi}{8}\right] \exp\left[-\frac{i\pi}{8}(\sigma_x^1 \sigma_x^2 + \sigma_y^1 \sigma_y^2 + \sigma_z^1 \sigma_z^2)\right] \quad (8)$$

where the σ^i 's are the usual Pauli spin matrices for the two on-site qubits

$$\sigma_x^k = \begin{pmatrix} 0 & 1 \\ 1 & 0 \end{pmatrix}, \quad \sigma_y^k = \begin{pmatrix} 0 & -i \\ i & 0 \end{pmatrix}, \quad \sigma_z^k = \begin{pmatrix} 1 & 0 \\ 0 & -1 \end{pmatrix}, \quad k=1,2 \quad (9)$$

It should be noted that \hat{U}^4 is the identity matrix, so that $\hat{U}^4|\nu\rangle = |\nu\rangle$.

The unitary streaming operator \hat{S}_1 acts on the qubit $|q_1\rangle$ at each lattice site and shifts it to the right to the next spatial node. The qubit $|q_2\rangle$ is not streamed by \hat{S}_1 . Thus the total collision matrix \hat{C} (which independently couples the two on-site qubits at each lattice site) does not commute with the global streaming operators \hat{S}_1 (which streams the 1st qubit at each lattice site to its nearest neighbor on the right). The algorithm is symmetrized by also introducing the global streaming operator \hat{S}_2 which performs a shift to the right of the 2nd qubit.

The appropriate collide-stream sequence of unitary operators needed to recover the dispersive part of NLS is dictated by the fact that $\hat{C}^4 = I$

$$\psi(t + \Delta t) = \hat{S}_2^T \hat{C} \hat{S}_2 \hat{C} \hat{S}_2^T \hat{C} \hat{S}_2 \hat{C} \hat{S}_1^T \hat{C} \hat{S}_1 \hat{C} \hat{S}_1^T \hat{C} \hat{S}_1 \hat{C} \psi(t) \quad (10)$$

where \hat{S}_i^T is the transpose of \hat{S}_i , with $\hat{S}_i^T \hat{S}_i = I$, $i=1,2$. Note that the potential in Eq. (1) can be readily introduced into the formalism by introducing a local phase change to the system wave function for each on-site qubit pair^{8,7} after performing the collide-stream sequence, Eq. (10):

$$\psi \rightarrow \text{Exp}[i\sigma V[|\psi\rangle] \Delta t] \psi, \quad \text{with } \sigma = \pm 1. \quad (11)$$

To proceed to the continuum limit one introduces the following scaling:

the spatial shift between neighboring lattice sites = $O(\varepsilon)$

$$\text{time advancement following stream-collide-phase sequence, Eqs. (10) and (11), } \Delta t = O(\varepsilon^2) \quad (12)$$

potential phase shift $V[|\psi\rangle] = O(\varepsilon^2)$

In the limit $\varepsilon \rightarrow 0$, it can be shown (using a symbolic manipulation program like *Mathematica*), that the collide-stream-phase sequence, Eqs. (10) and (11), under the ordering Eq. (12) yields the NLS equation – with arbitrary potential V –

$$i \frac{\partial \psi}{\partial t} + \frac{\partial^2 \psi}{\partial x^2} + \sigma V[|\psi\rangle] \psi = 0 + O(\varepsilon^2), \quad \text{with } \sigma = \pm 1. \quad (13)$$

2.2 Vector NLS

To recover the vector NLS equations appropriate for the study of polarized solitons and two-species BEC

$$\begin{aligned} i \frac{\partial \psi_1}{\partial t} + \frac{\partial^2 \psi_1}{\partial x^2} + \sigma_1 V_1[|\psi_1\rangle, |\psi_2\rangle] \psi_1 &= 0 \\ i \frac{\partial \psi_2}{\partial t} + \frac{\partial^2 \psi_2}{\partial x^2} + \sigma_2 V_2[|\psi_1\rangle, |\psi_2\rangle] \psi_2 &= 0 \end{aligned} \quad (14)$$

we now introduce at each lattice site 2 qubits for ψ_1 and 2 qubits for ψ_2 . The collide-stream sequence of unitary operators is applied simultaneously (and independently) to the qubit pairs $|q_1, q_2\rangle$ and $|q_3, q_4\rangle$ since the interaction between the wave functions ψ_1 and ψ_2 occurs only through the potentials $V_i[|\psi_1|, |\psi_2|]$:

$$\begin{pmatrix} \psi_1(t + \Delta t) \\ \psi_2(t + \Delta t) \end{pmatrix} = \begin{pmatrix} \hat{S}_2^T \hat{C} \hat{S}_2 \hat{C} \hat{S}_2^T \hat{C} \hat{S}_2 \hat{C} \hat{S}_1^T \hat{C} \hat{S}_1 \hat{C} \hat{S}_1^T \hat{C} \hat{S}_1 \hat{C} \\ \hat{S}_2^T \hat{C} \hat{S}_2 \hat{C} \hat{S}_2^T \hat{C} \hat{S}_2 \hat{C} \hat{S}_1^T \hat{C} \hat{S}_1 \hat{C} \hat{S}_1^T \hat{C} \hat{S}_1 \hat{C} \end{pmatrix} \begin{pmatrix} \psi_1(t) \\ \psi_2(t) \end{pmatrix} \quad (15)$$

with

$$\begin{pmatrix} \psi_1 \\ \psi_2 \end{pmatrix} \rightarrow \begin{pmatrix} \text{Exp}[i \sigma_1 V_1[|\psi_1|, |\psi_2|] \Delta t] \\ \text{Exp}[i \sigma_2 V_2[|\psi_1|, |\psi_2|] \Delta t] \end{pmatrix} \begin{pmatrix} \psi_1 \\ \psi_2 \end{pmatrix} \quad (16)$$

3. NUMERICAL SIMULATIONS USING THE QUANTUM LATTICE ALGORITHM

3.1 Scalar Dark Solitons

The quantum lattice algorithm Eqs. (10) and (11), for the case of the black soliton solution to the defocusing NLS

$$i \frac{\partial \psi}{\partial t} + \frac{\partial^2 \psi}{\partial x^2} - 2|\psi|^2 \psi = 0 \quad (17)$$

is shown in Fig. 3 for initial parameters $a=0.01$, $x_0 = 100$ and times $t=100, 200$. The maximal pointwise divergence from the exact solution, Eq. (1), at $t=200$ is typically less than 0.05%.

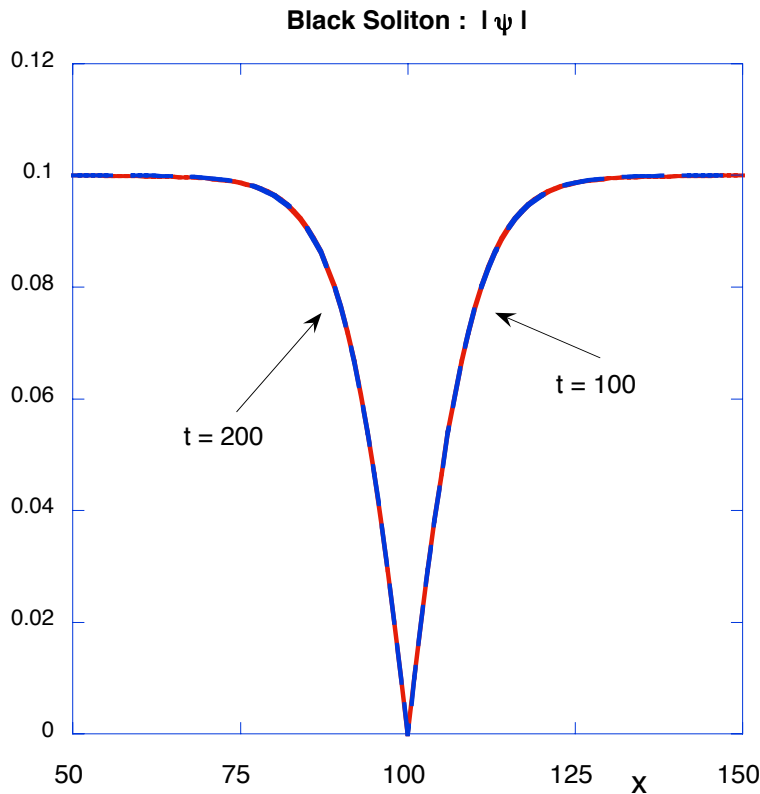


Fig. 3 Quantum Lattice solution $|\psi|$ of the stationary black soliton for defocusing NLS. The surface plot is shown in Fig. 1

The corresponding quantum lattice algorithm, Eqs. (10) and (11), for the dark-dark soliton collision is shown in Fig. 4 for initial parameters: $x_0 = 500$, $t_0 = -500$ and $a = \sqrt{2}/10$.

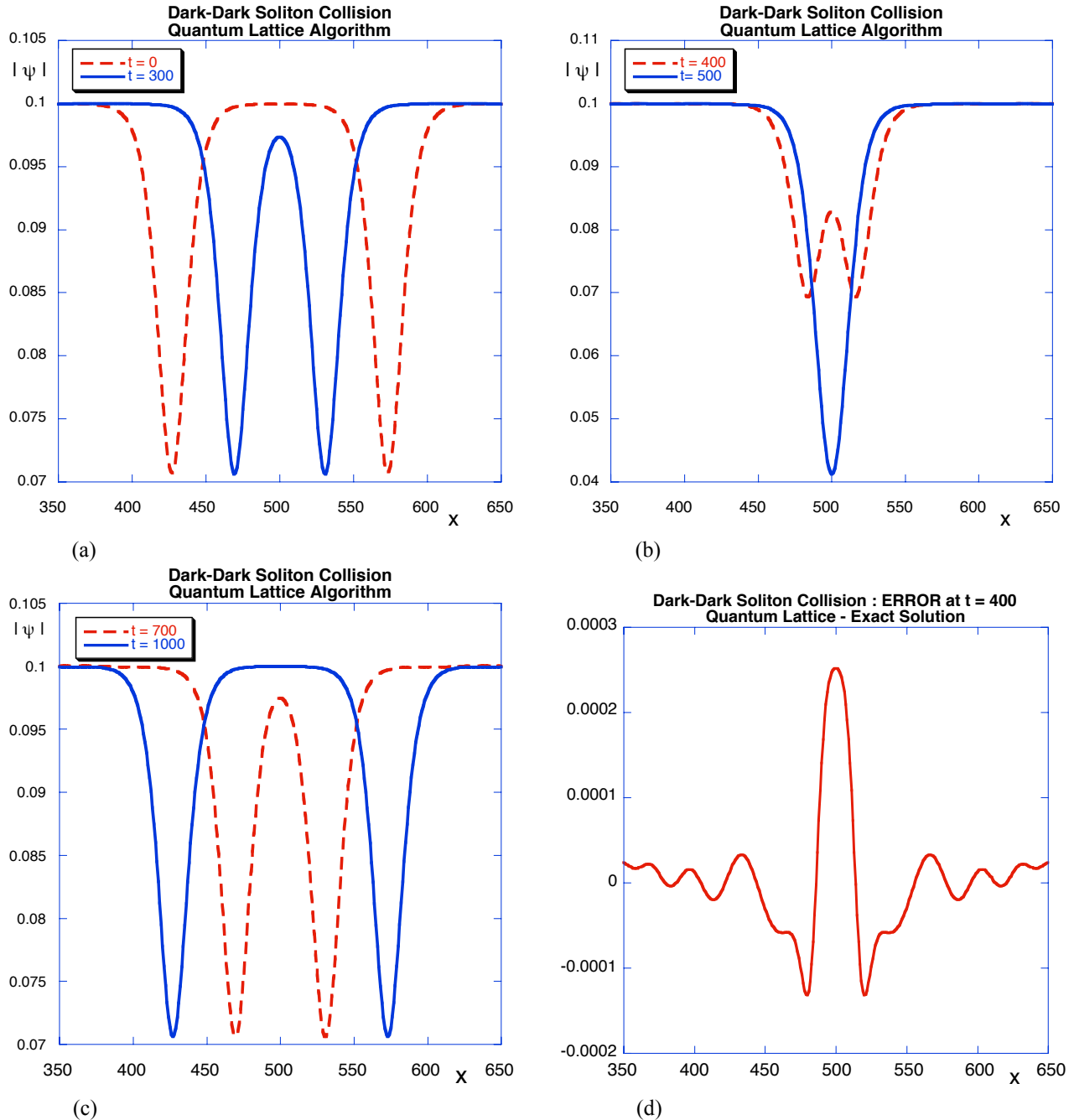


Fig. 4 The quantum lattice algorithm for the dark-dark soliton solution for the defocusing NLS, Eq. (17) with initial conditions : $x_0 = 500$, $t_0 = -500$, $a = \sqrt{2}/10$. (a) Plot of $|\psi|$ for $t = 0$ and $t = 300$ as the dark solitons approach each other, (b) at $t = 400$ and $t = 500$ there is strong overlap followed by separation as the dark solitons pass through each other, (c) times $t = 700$ and $t = 1000$. (d) the difference $|\psi(x, t = 400)|_{\text{quantum}} - |\psi(x, t = 400)|_{\text{exact}}$ in the absolute values of the wave function at $t = 400$. The quantum simulation is on a very coarse grid of only a 1000 spatial nodes and the algorithm takes less than 3 s to complete 1000 time iterations on a MAC G5 in double precision. The surface plot of this dark-dark soliton collision is shown in Fig. 2 The symmetry in the error plot (d) indicates a very balanced algorithm.

As a final example of the use of our quantum lattice algorithm we consider the motion of a coupled dark-bright soliton in a vector defocused NLS system⁶. For self-defocused NLS, the bright soliton *per se* is not a solution, so that this initial profile will undergo spatial dispersion, Fig. 5(a). However such a bright soliton *can* exist in self-defocused NLS when it is trapped within a co-propagating dark soliton. The vector self-defocusing NLS equations are

$$\begin{aligned} i \frac{\partial \psi_D}{\partial t} + \frac{\partial^2 \psi_D}{\partial x^2} - \left[|\psi_B|^2 + |\psi_D|^2 - \mu \right] \psi_D &= 0 \\ i \frac{\partial \psi_B}{\partial t} + \frac{\partial^2 \psi_B}{\partial x^2} - \left[|\psi_B|^2 + |\psi_D|^2 - \mu \right] \psi_B &= 0 \end{aligned} \quad (18)$$

with exact dark soliton wave function ψ_D , and bright soliton wave function ψ_B solutions⁶

$$\begin{aligned} \psi_D(x,t) &= i\sqrt{\mu} \text{Sin} \alpha + \sqrt{\mu} \text{Cos} \alpha \cdot \text{Tanh} \left[\kappa \left(\frac{x}{\sqrt{2}} - x_0 - t \kappa \text{Tan} \alpha \right) \right], \\ \psi_B(x,t) &= \sqrt{\frac{N_B \kappa}{2}} \text{Exp} \left[i \frac{\kappa^2 (1 - \text{Tan}^2 \alpha)}{2} t + i \frac{x}{\sqrt{2}} \kappa \text{Tan} \alpha \right] \text{Sech} \left[\kappa \left(\frac{x}{\sqrt{2}} - x_0 - t \kappa \text{Tan} \alpha \right) \right] \end{aligned} \quad (19)$$

In the terminology of BEC, μ corresponds to the chemical potential, N_B is the rescaled number of particles in the bright soliton state, and the soliton inverse length is

$$\kappa = \sqrt{\mu \text{Cos}^2 \alpha + \frac{N_B^2}{16} - \frac{N_B}{4}}$$

The co-propagating dark-bright soliton pair has velocity $\sqrt{2} \kappa \text{Tan} \alpha$.

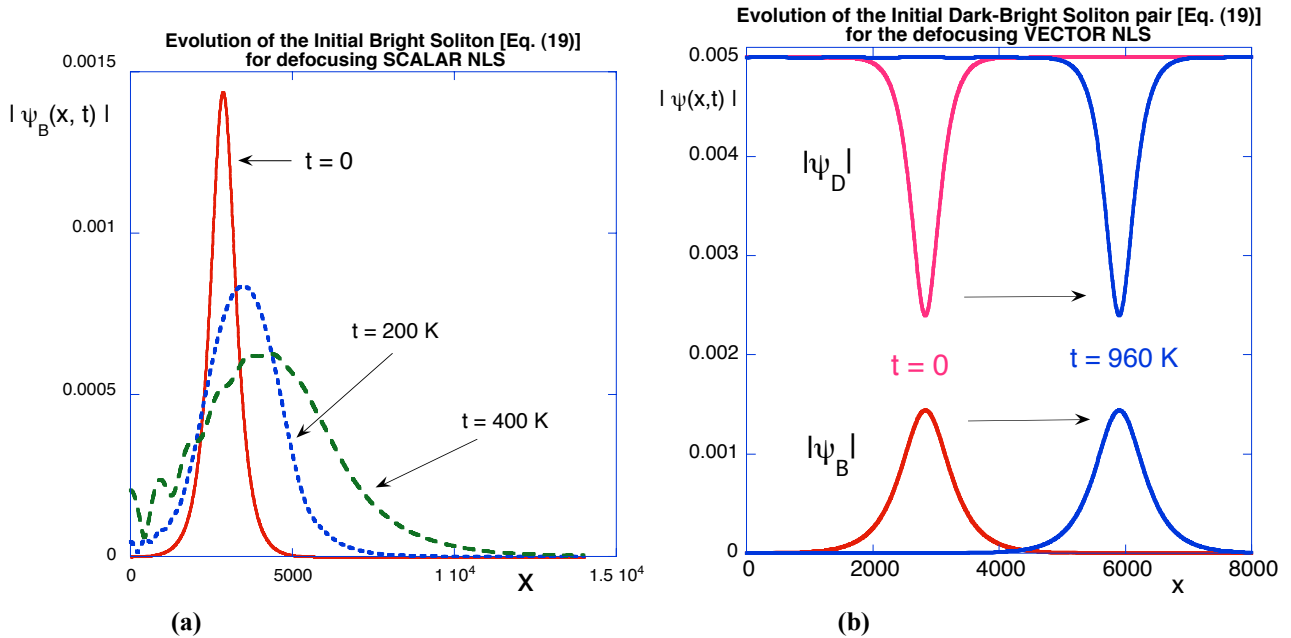


Fig. 5 (a) For the defocusing scalar NLS, the initial profile of a bright soliton diffuses since stationary solutions of the defocusing NLS are dark solitons. **(b)** For vector defocusing NLS, with initial profiles of a bright-dark soliton pair [Eq. (19) with $t = 0$], the propagating dark soliton traps the bright soliton and prevents its decay even in the defocusing case. The parameters for these runs are $\mu = 0.000025$, $N_B = 0.001$, $\alpha = 0.5$ on a spatial grid of 14000 and 960 K time iterations.

In Fig. 6 we compare the real and imaginary parts of the dark soliton wave function ψ_D at $t = 480$ K and 960 K to the exact solution (19). There is little error in the $\text{Re}[\psi_{QL} - \psi_{exact}]_{\text{DARK}}$, as seen Fig. 6 (a). However, the numerical noise

in $\text{Im}[\psi_{QL} - \psi_{exact}]_{DARK}$ at $t = 480$ K, Fig. 6 (b), has increased by two orders of magnitude into structured oscillations which eventually will disrupt the simulation.

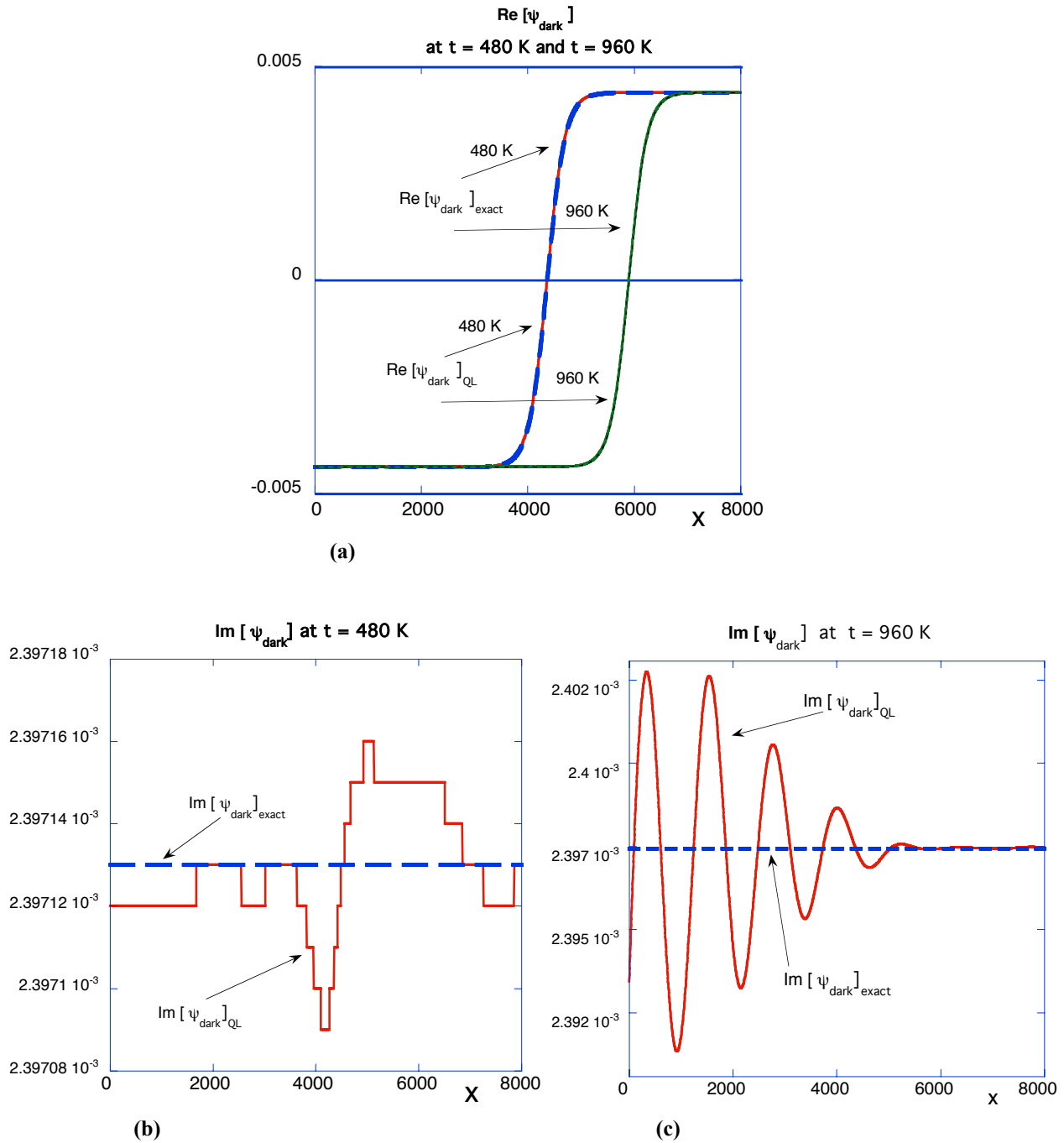


Fig. 6 A plot of (a) $\text{Re}[\psi_{dark}]_{QL}$ and $\text{Re}[\psi_{dark}]_{exact}$ at $t = 480$ K and $t = 960$ K. Even at $t = 960$ K, the relative error is less than 0.07%. $\text{Im}[\psi_{dark}]_{QL}$ and $\text{Im}[\psi_{dark}]_{exact} = \text{const.}$ at (b) $t = 480$ K, (c) $t = 960$ K. The extremely low numerical noise at $t = 480$ K (errors $< 0.002\%$) has been amplified to structured oscillations with errors $< 0.2\%$. The (theoretical) phase discontinuity of ψ_{dark} about its minimum is 0.71π [see (a) – (c)].

4. DISCUSSION AND COMMENTS

We have extended our quantum lattice algorithm to now cover both the self-focusing and self-defocusing NLS. While this is accomplished by a simple sign flip in the nonlinear potential term, the effect on the soliton solution is quite dramatic. In particular, the bright soliton complex wave function ψ_B (an exact solution to the cubic self-focusing NLS) does not have a phase jump across its maximum. Numerically this permits the use of periodic boundary conditions in the quantum lattice algorithm.^{3,4} On the other hand, there is a phase discontinuity of π at the zero intensity minimum of a black soliton complex wave function. As a result we abandoned the imposition of standard periodic boundary conditions and employed inflow streaming boundary conditions using EOShift

The numerical solution of the defocusing NLS for dark solitons is also plagued by the occurrence of numerical (round-off) instabilities. Numerical noise hits both the standard split-step Fourier method as well as the quantum lattice method. Parameters have to be chosen so that the physics of interest is achieved before these numerical instabilities hit.

The interplay between BEC and solitons has become an extremely active research area. In particular, the 3D Gross-Pitaevskii (GP) equation:

$$i\hbar \frac{\partial \psi(\mathbf{r}, t)}{\partial t} = \left[-\frac{\hbar^2}{2m} \nabla^2 + U(\mathbf{r}) + g N_c |\psi(\mathbf{r}, t)|^2 \right] \psi(\mathbf{r}, t) \quad (20)$$

is a mean field theory of the macroscopic wave function $\psi(\mathbf{r}, t)$ of the Bose-Einstein condensate. $U(\mathbf{r})$ is the external trapping potential, $g = 4\pi \hbar^2 a_s / m$ is the scattering amplitude with a_s the s-wave scattering length, and N is proportional to the number of condensed bosons. The GP mean field theory has been very successful in describing experimental results on dilute Bose-Einstein condensates near zero temperature. Of much interest, both experimentally and theoretically, is the reduced dimension description of BEC as one experimentally constricts the condensate to disk-shaped objects. In appropriate trapping potentials, Salasnich et. al¹¹ have derived a 1D nonpolynomial NLS for the condensate of the form

$$i\hbar \frac{\partial \phi}{\partial t} = \left[-\frac{\hbar^2}{2m} \frac{\partial^2}{\partial x^2} + V(x) + \frac{gN}{2\pi a_{\perp}^2} \frac{|\phi|^2}{\sqrt{1+2a_s N |\phi|^2}} + \frac{\hbar \omega_{\perp}}{2} \left(\sqrt{1+2a_s N |\phi|^2} + \frac{1}{\sqrt{1+2a_s N |\phi|^2}} \right) \right] \phi \quad (21)$$

where $a_{\perp} = \sqrt{\hbar / m \omega_{\perp}}$ is the oscillator strength in the transverse direction and $\psi(\mathbf{r}, t) = \psi_{\perp}(y, z, t) \phi(x, t)$. In the special case of weakly interacting Bose particles, $a_s N |\phi|^2 \ll 1$, Eq. (21) reduces to a cubic NLS with external potential V :

$$i\hbar \frac{\partial \phi}{\partial t} = \left[-\frac{\hbar^2}{2m} \frac{\partial^2}{\partial x^2} + V(x) + \frac{gN}{2\pi a_{\perp}^2} |\phi|^2 \right] \phi$$

while in the limit of strongly interacting axial high-density condensate $a_s N |\phi|^2 \gg 1$ (but with overall 3D dilute condensate $a_s N |\psi|^2 \ll 1$), reduces to the quadratically nonlinear NLS

$$i\hbar \frac{\partial \phi}{\partial t} = \left[-\frac{\hbar^2}{2m} \frac{\partial^2}{\partial x^2} + V(x) + \frac{3}{2} \frac{gN^{1/2}}{2\pi a_{\perp}^2 \sqrt{2a_s}} |\phi| \right] \phi$$

We intend to consider these equations as well as the full 3D GP equation using quantum lattice algorithms.

ACKNOWLEDGMENTS

This work was supported by the Directorate of Computational Mathematics, Air Force Office of Scientific Research.

REFERENCES

- [1] Y. S. Kivshar and G. P. Agrawal, *Optical Solitons – from fibers to photonic crystals*, Academic Press, London, 2003
- [2] S. Inouye, M. R. Andrews, J. Stenger, H. –J. Miesner, D. M. Stamper-Kurn and W. Ketterle, “Observation of Feshbach resonances in a Bose-Einstein condensate”, *Nature* **392**, 575-579 (1998)
- [3] G. Vahala, L. Vahala and J. Yepez, “Quantum lattice gas representation of some classical solitons”. *Phys. Lett. A* **310**, 387-396 (2003)
- [4] G. Vahala, L. Vahala and J. Yepez, “Quantum lattice gas representation of vector solitons”, *SPIE Conf. Proc.* **5105**, 273-281 (2003)
- [5] N. Akhmediev and A. Ankiewicz, “First-order exact solutions of the nonlinear Schrodinger equation in the normal-dispersion regime”, *Phys. Rev. A* **47**, 3213-3221 (1993)
- [6] Th. Busch and J. R. Anglin, “Dark-bright solitons in inhomogeneous Bose-Einstein condensates,” *Phys. Rev. Lett.* **87**, 010401 (2001)
- [7]] J. Yepez and B. M. Boghosian, “An efficient and accurate quantum lattice-gas model for the many-body Schrodinger wave equation”., *Comp. Phys. Comm.*, **146**, 280-294 (2002)
- [8] I. Bialynicki-Birula, “Weyl, Dirac, and Maxwell equations on a lattice as unitary cellular automata”, *Phys. Rev. D* **49**, 6920-6927 (1994)
- [9] Th. Busch and J. R. Anglin, “Mossbauer effect for dark solitons in Bose-Einstein condensates”, *to be published* [arXiv:cond-mat/9809408, revised Dec. 22, 2003]
- [10] Th. Busch and J. R. Anglin, “Motion of dark solitons in trapped Bose-Einstein condensates”, *Phys. Rev. Lett* , **84**, 2298-2301, (2000).
- [11] L. Salasnich, A. Parola and L. Reatto, “Effective wave equations for the dynamics of cigar-shaped and disk-shaped Bose condensates”, *Phys. Rev. A* **65**, 043614 (2002)